

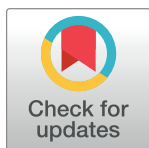
RESEARCH ARTICLE

Comparison of the binding of the gastrin-releasing peptide receptor (GRP-R) antagonist ^{68}Ga -RM2 and ^{18}F -FDG in breast cancer samples

Clément Morgat^{1,2,3*}, Romain Schollhammer^{1,2,3}, Gaétan Macgrogan^{4,5}, Nicole Barthe⁶, Valérie Vélasco^{4,5}, Delphine Vimont^{2,3}, Anne-Laure Cazeau⁷, Philippe Fernandez^{1,2,3}, Elif Hindie^{1,2,3}

1 Nuclear Medicine Department, University Hospital of Bordeaux, Bordeaux, France, **2** Univ. Bordeaux, INCIA, UMR-CNRS 5287, Talence, France, **3** CNRS, INCIA, UMR 5287, Talence, France, **4** Surgical Pathology Unit, Department of BioPathology, Institut Bergonié, Bordeaux, France, **5** INSERM, ACTION U1218, Bordeaux, France, **6** BioTis, INSERM U1026, Bordeaux, France, **7** Nuclear Medicine Department, Institut Bergonié, Bordeaux, France

* clement.morgat@u-bordeaux.fr



OPEN ACCESS

Citation: Morgat C, Schollhammer R, Macgrogan G, Barthe N, Vélasco V, Vimont D, et al. (2019) Comparison of the binding of the gastrin-releasing peptide receptor (GRP-R) antagonist ^{68}Ga -RM2 and ^{18}F -FDG in breast cancer samples. PLoS ONE 14(1): e0210905. <https://doi.org/10.1371/journal.pone.0210905>

Editor: Aamir Ahmad, University of South Alabama Mitchell Cancer Institute, UNITED STATES

Received: October 15, 2018

Accepted: January 3, 2019

Published: January 15, 2019

Copyright: © 2019 Morgat et al. This is an open access article distributed under the terms of the [Creative Commons Attribution License](https://creativecommons.org/licenses/by/4.0/), which permits unrestricted use, distribution, and reproduction in any medium, provided the original author and source are credited.

Data Availability Statement: All relevant data are within the manuscript and its Supporting Information files.

Funding: This study was funded by "La ligue contre le Cancer Gironde".

Competing interests: The authors have declared that no competing interests exist.

Abstract

The Gastrin-Releasing Peptide Receptor (GRPR) is over-expressed in estrogen receptor (ER) positive breast tumors and related metastatic lymph nodes offering the opportunity of imaging and therapy of luminal tumors. ^{68}Ga -RM2 binding and ^{18}F -FDG binding in tumoral zones were measured and compared using tissue micro-imaging with a beta imager on 14 breast cancer samples (10 primaries and 4 associated metastatic lymph nodes). Results were then assessed against ER expression, progesterone receptor (PR) expression, HER2 over-expression or not and Ki-67 expression. GRPR immunohistochemistry (IHC) was also performed on all samples. We also retrospectively compared ^{68}Ga -RM2 and ^{18}F -FDG bindings to ^{18}F -FDG SUV_{max} on the pre-therapeutic PET/CT examination, if available. ^{68}Ga -RM2 binding was significantly higher in tumors expressing GRPR on IHC than in GRPR-negative tumors ($P = 0.022$). In ER⁺ tumors, binding of ^{68}Ga -RM2 was significantly higher than ^{18}F -FDG ($P = 0.015$). In tumors with low Ki-67, ^{68}Ga -RM2 binding was also significantly increased compared to ^{18}F -FDG ($P = 0.029$). Overall, the binding of ^{68}Ga -RM2 and ^{18}F -FDG displayed an opposite pattern in tumor samples and ^{68}Ga -RM2 binding was significantly higher in tumors that had low ^{18}F -FDG binding ($P = 0.021$). This inverse correlation was also documented in the few patients in whom a ^{18}F -FDG PET/CT examination before surgery was available. Findings from this in vitro study suggest that GRPR targeting can be an alternative to ^{18}F -FDG imaging in ER⁺ breast tumors. Moreover, because GRPR antagonists can also be labeled with lutetium-177 this opens new avenues for targeted radionuclide therapy in the subset of patients with progressive metastatic disease following conventional treatments.

Introduction

The Gastrin-Releasing Peptide Receptor (GRPR, also named BB2) is a G-protein coupled receptor of the bombesin family. Its over-expression on the membrane of tumor cells offers the opportunity of a selective targeting, using suitable radiolabelled bioconjugates, for positron emission tomography (PET) imaging and targeted radionuclide therapy (TRT). Tumors that can be targeted with GRPR-based radiotracers are notably, prostate cancer, breast cancer, lung cancer and colorectal cancer among others [1]. We have recently studied, using immunohistochemistry, the expression of GRPR in a large series of primary breast cancers and found that GRPR was overexpressed in 83.2% of ER-positive tumors but only in 12% of ER-negative tumors ($p < 0.00001$) [2]. When examined in molecular subtypes, GRPR is over-expressed in 86.2% of luminal-A and 82.8% of luminal-B HER2 negative tumors while triple negative breast cancers and HER2-enriched phenotypes exhibit GRPR over-expression in only 7.8% and 21.3% of cases. Importantly, lymph nodes metastases of GRPR-positive tumors also showed GRPR overexpression [2]. The association between GRPR and ER has also been documented at mRNA level by Dalm and colleagues [3]. Recently, GRP-R antagonists radiolabelled for PET imaging, demonstrated promising results in breast cancer patients. For example, in a small pilot study that used ^{68}Ga -SB3, metastases were successfully visualized in 4 out of 6 patients [4]. In another study, ^{68}Ga -RM2 could image with high contrast 13/18 primary breast tumors and detected metastatic lesions [5]. In a more recent study conducted in 34 women with suspected breast cancer, a novel GRPR antagonist, ^{68}Ga -NOTA-RM26, was able to delineate primary breast tumors in 29/34 patients and lymph nodes metastases in 15/18 patients with node-positive disease [6]. Comparison of breast cancer imaging using GRP-R based radioantagonists and ^{18}F -FDG is now needed to elucidate the place of GRP-R in the complex landscape of breast cancer imaging. This *in vitro* study aimed to assess the binding of ^{18}F -FDG and that of the GRPR antagonist ^{68}Ga -RM2 on representative breast cancer samples.

Materials and methods

Breast cancer samples

This study was approved by our institutional review board “Institut Bergonié Groupe Sein”. The project and data collection were performed according to the national French commission on informatics and liberty (CNIL). Prior to surgery, patients had given written consent to the use of part of the tumor material for research, after diagnostic procedures had been performed. Fourteen samples of formalin-fixed, paraffin-embedded breast cancer tissues (10 primary tumors and 4 associated metastatic lymph nodes) were retrospectively selected at Institut Bergonié. Sample characteristics are presented in Table 1. No patients had received neoadjuvant hormone therapy or chemotherapy. For each case, 6 successive slices were used: 1 for HES staining, 1 for GRP-R immunohistochemistry and 4 for micro-imaging of tissue radioactivity (one slice per radiopharmaceutical for total binding and one slice per radiopharmaceutical for non-specific binding). GRP-R immunohistochemistry was carried-out as previously described [2].

Immunohistochemistry. IHC analyses were performed on 3 μm tumor sections using specific antibodies directed against ER, PR, HER2/neu, Ki-67 and GRPR. All immunohistochemical techniques were performed on a Roche Ventana Benchmark ultra-automat. Details of antibody clones, manufacturers, dilutions used, incubation times, pretreatment buffers and staining kits are summarized in Table 2.

Nuclear staining was assessed for ER and PR. A negative ER and/or PR status was defined by the presence of less than 1% of positive tumor cells. HER2/neu staining was scored according to the ASCO/CAP 2013 recommendations [7]. Ki-67 index was assessed semi-

Table 1. Estrogen receptor (ER), progesterin receptor (PR) expression, HER2 status, Ki-67 expression, molecular phenotypes and Gastrin-Releasing Peptide Receptor (GRP-R) expression in our series of samples.

Sample	ER (%)	PR (%)	HER2 over-expression	Ki-67 (%)	Molecular phenotype	GRPR status
Primary tumors						
1	70	90	No	2	Luminal-A	Pos
2	90	90	No	5	Luminal-A	Pos
3	80	30	No	20	Luminal-B	Pos
4	100	30	No	50	Luminal-B	Pos
5	90	0	No	30	Luminal-B	Neg
6	100	100	No	15	Luminal-B	Pos
7	0	0	Yes	20	HER2-enriched	Pos
8	0	0	Yes	35	HER2-enriched	Pos
9	0	0	Yes	25	Molecular apocrine	Pos
10	0	0	No	70	Basal	Neg
Metastatic lymph nodes						
11 from tumor 2	100	100	No	15	n.a. (not applicable)	Pos
12 from tumor 5	100	1	No	60	n.a.	Pos
13 from tumor 7	0	0	No	50	n.a.	Pos
14 from tumor 9	0	0	No	40	n.a.	Pos

<https://doi.org/10.1371/journal.pone.0210905.t001>

quantitatively and was considered low when 19% or less of tumor cell nuclei were stained and high when 20% or more tumor cell nuclei were stained. Molecular subtypes of breast cancers were derived from immunohistochemical markers (based on ER status, progesterone receptor PgR status, Ki-67 labeling index and HER2 status) according to St Gallen consensus [8] and Maisonneuve classification [9]. Molecular subtypes were defined as follows: Luminal A-like (HER2-, ER ≥ 1% and Ki-67 < 14% or Ki-67 ranging from 14% to 19% and PgR ≥ 20%); Luminal B-like HER2- (HER2-, ER ≥ 1% and Ki-67 ≥ 20% or Ki-67 14%–19% and PgR < 20%); Luminal B-like HER2+ (HER2+, ER ≥ 1%); HER-2 enriched (HER2+, ER = 0% and PgR = 0%); Triple-negative (ER = 0%, PgR = 0%, HER2-).

Results for GRP-R immunohistochemistry were expressed as previously described [2]. An experimented pathologist (GMG) quantified GRP-R expression and manually drew tumoral regions on the HES slice for quantification.

⁶⁸Ga-RM2 radiosynthesis and quality controls. Radiolabelling experiments were performed on an automated synthesizer (GE FastLab, GE Healthcare, GEMS Benelux, Belgium). Briefly, 40µg of RM2 (Life Molecular Imaging) was heated at 90 °C during 5min using microwaves with 1.1 mL ⁶⁸GaCl₃ (GalliEo generator with nominal activity of 1850 MBq, IRE Elit,

Table 2. Characteristics of antibodies used in this study.

Antibody	Clone	Supplier	Dilution	Incubation time	Unmasking	Revelation
ER	SP1	Roche Diagnostics (760–4605)	Ready to use	32 min	CC1 standard (64')	UltraView Universal DAB
PR	1E2	Roche Diagnostics (790–4296)	Ready to use	12 min	CC1 short (36')	UltraView Universal DAB
HER2	4B5	Roche Diagnostics (790–4493)	Ready to use	12 min	CC1 short (36')	UltraView Universal DAB
Ki-67	30.9	Roche Diagnostics (790–4493)	Ready to use	32 min	CC1 standard (64')	UltraView Universal DAB
GRP-R	polyclonal	Origene Technologies Rockville, Maryland	1/800	52 min	Protease 1 (4 min)	UltraView Universal DAB

<https://doi.org/10.1371/journal.pone.0210905.t002>

Belgium) and 5mg of ascorbic acid. The raw solution was then purified on a C_{18} cartridge (WAT023501) preconditioned with 1mL ethanol (Merck) and 5 mL water (GE Healthcare). The final product was then eluted with 1 mL ethanol and formulated in PBS. ^{68}Ga -RM2 was checked for radiochemical purity using HPLC (Phenomenex Luna C_{18} ; 250mm x 4.6mm x 5 μm ; 2.5 mL/min, $\lambda = 220\text{nm}$). The analytical HPLC system used was a JASCO system with ChromNAV software, a PU-2089 Plus quaternary gradient pump, a MD-2018 Plus photodiode array detector and Raytest Gabi Star detector. Amount of ^{68}Ga -RM2 was determined by UV-HPLC by linear regression of the calibration curve established using the reference compound $^{\text{nat}}\text{Ga}$ -RM2 (Life Molecular Imaging).

Tracer incubation and tissular micro-imaging. After dewaxing, rehydration and unmasking, samples were pre-incubated during 10min at 37°C in Tris-HCl buffer at pH 7.4. Then, binding solution containing 5nM of ^{68}Ga -RM2 or 1MBq (amount of ^{18}F -FDG is not determined by the supplier) of ^{18}F -FDG in Tris-HCl buffer pH 8.2, containing 1% of BSA (Sigma-Aldrich), 40 $\mu\text{g}/\text{mL}$ of bacitracin (Sigma-Aldrich) and 10nM of MgCl_2 (Sigma-Aldrich) was applied. To assess non-specific binding, 1 μM of reference compounds $^{\text{nat}}\text{Ga}$ -RM2 or $^{\text{nat}}\text{F}$ -FDG was added in adjacent slices. Samples were then incubated at 37°C for 2 hours. Afterwards, samples were rinsed 5 times during 8min in cold Tris-HCl buffer at pH 8.2 with 0.25% of BSA, 2 times during 8 minutes in cold Tris-HCl buffer at pH 8.2 without BSA and finally 2 times during 5 minutes in distilled water. Finally, samples were dried using air stream and were imaged using a beta imager 2000 (Biospace Lab).

Signal quantification. The M3Vision software was used for signal quantification. Total binding and non-specific binding were determined using the region of interest (ROI) method. First, a manual fusion by affine transformation of homologous structures was performed using the HES slice to match the radioactivity distribution to histology. Afterwards, on the total binding image (^{68}Ga -RM2 or ^{18}F -FDG alone) a first ROI (tumoral ROI) was placed on the tumoral zone and a second ROI (noise ROI), corresponding to noise, was placed around the tissue. Then, the same ROIs were applied on quantitative images from adjacent slices representing non-specific binding (^{68}Ga -RM2 or ^{18}F -FDG plus excess of reference compound) to define non-specific binding. Finally, data were exported on Excel software for processing. Parameters “Signal to Noise Ratio (SNR)” and “Delta” were then calculated. SNR was defined as the signal in tumoral ROI minus signal in noise ROI. Delta was calculated as follow:

$$\text{Delta}(\%) = \frac{\text{SNR}_{\text{total binding}} - \text{SNR}_{\text{non specific binding}}}{\text{SNR}_{\text{total binding}}} \times 100$$

Statistical analysis. Differences between mean values were assessed using non parametric t-test. A *P*-value of less than 0.05 was considered statistically significant. Statistical analysis was performed using GraphPad Prism software v 6.01.

Retrospective analysis of ^{18}F -FDG PET/CT. We retrospectively analyzed pre-therapeutic ^{18}F -FDG PET/CT performed at the Nuclear Medicine Department of Institut Bergonié. PET/CT had been performed before surgery in only 2 patients, corresponding to tissue samples 1 and 5 in Table 1. ^{18}F -FDG uptake was measured as SUV_{max} in a VOI drawn on the breast tumor.

Results

^{68}Ga -RM2 radiosynthesis

^{68}Ga -RM2 was obtained at a mean specific activity of $47.3 \pm 16.7 \text{ GBq}/\mu\text{mol}$ and a mean radiochemical purity of $99.52 \pm 0.18\%$ suitable for *in vitro* experiments.

Comparison of ^{68}Ga -RM2 binding and GRP-R immunohistochemistry

As a validation step we assessed whether tissular micro-imaging may accurately reflect IHC results. We stratified samples according to their GRP-R status determined by IHC and our results showed that the mean ^{68}Ga -RM2 delta was significantly higher in GRP-R expressing tumors than in GRP-R-negative tumors ($33.93 \pm 17.55\%$ vs $0.0 \pm 0.0\%$; $P = 0.022$).

^{68}Ga -RM2 and ^{18}F -FDG bindings

Qualitative analysis. Qualitative analysis showed a good signal-to-noise ratio, and a binding in agreement with GRPR IHC with clear differences between total and non-specific bindings (Fig 1).

Quantitative analysis: Association between ^{68}Ga -RM2 and ^{18}F -FDG bindings and biological data. There was a significantly higher specific binding of ^{68}Ga -RM2 in the ER⁺ group vs ER⁻ tumors ($45.31 \pm 13.23\%$ vs $14.32 \pm 9.20\%$; $P = 0.030$). Contrarily, there was a trend for lower ^{18}F -FDG uptake in ER⁺ tumors ($16.51 \pm 28.45\%$ vs $20.21 \pm 17.77\%$ $P = 0.479$).

There was also a higher specific binding of ^{68}Ga -RM2 in the PR⁺ groups vs PR⁻ tumors ($43.29 \pm 13.24\%$ vs $18.18 \pm 18.43\%$; $P = 0.028$). Contrarily, ^{18}F -FDG uptake looked similar in PR⁺ and PR⁻ tumors ($21.70 \pm 31.90\%$ vs $21.13 \pm 18.24\%$; $P = 0.730$).

A striking difference in ^{68}Ga -RM2 binding was seen according to the percentage of Ki-67 staining. ^{68}Ga -RM2 binding was significantly higher in the low Ki-67 group ($49.24 \pm 9.15\%$ vs $20.62 \pm 17.88\%$; $P = 0.023$). Contrarily so, there was a trend for higher ^{18}F -FDG uptake in the high Ki-67 group vs low Ki-67 group ($25.77 \pm 26.43\%$ vs $10.40 \pm 12.35\%$; $P = 0.287$).

There were no significant differences in the HER2⁺ and HER2⁻ groups for ^{68}Ga -RM2 or for ^{18}F -FDG binding (Table 3).

Quantitative analysis: Comparison of ^{68}Ga -RM2 and ^{18}F -FDG bindings. In ER⁺ tumors, binding of ^{68}Ga -RM2 was largely higher than ^{18}F -FDG ($45.31 \pm 13.23\%$ vs $16.51 \pm 28.45\%$; $P = 0.015$), while in ER⁻ tumors binding of ^{18}F -FDG was comparable to that of ^{68}Ga -RM2 ($P = 0.483$). Therefore, the ratio of mean ^{68}Ga -RM2 binding to ^{18}F -FDG was 3.42 in ER⁺ tumors vs 0.71 in ER⁻ tumors. There was also a strong trend for higher ^{68}Ga -RM2 binding than ^{18}F -FDG in PR⁺ tumors ($P = 0.089$) while no differences were observed in the PR⁻ group ($P = 0.626$). In these subgroups, the ratio of mean ^{68}Ga -RM2 binding to ^{18}F -FDG was 1.99 in PR⁺ tumors vs 0.86 in PR⁻ tumors. In tumors with low Ki-67, ^{68}Ga -RM2 binding was also significantly increased compared to ^{18}F -FDG ($49.24 \pm 9.15\%$ vs $10.40 \pm 12.35\%$; $P = 0.029$). There was no differences in the bindings of ^{68}Ga -RM2 and ^{18}F -FDG in tumors with high Ki-67 ($P = 0.783$). These differences translate in a higher ratio of mean ^{68}Ga -RM2 binding to ^{18}F -FDG in low Ki-67 tumors (4.73 vs 0.80). In HER2⁻ tumors, the ratio of mean ^{68}Ga -RM2 binding to ^{18}F -FDG was 1.70 while in HER2⁺ this ratio reaches only 0.53.

We also looked for ^{68}Ga -RM2 binding in tumors considered negatives for ^{18}F -FDG. Interestingly, ^{68}Ga -RM2 binding was significantly higher in ^{18}F -FDG-negative tumors: $36.03 \pm 21.31\%$ in ^{18}F -FDG negative tumors vs $9.75 \pm 11.06\%$ in ^{18}F -FDG-positive tumors, $P = 0.021$, S1 Fig.

^{18}F -FDG PET/CT

Among patients studied using tissular micro-imaging, two had undergone ^{18}F -FDG PET/CT imaging for staging before surgery (Table 4). The first patient had a low ^{18}F -FDG uptake *in vivo* ($\text{SUV}_{\text{max}} = 2.5$), a negative ^{18}F -FDG delta *ex vivo*, a high ^{68}Ga -RM2 delta of 37.46% and a positive GRP-R IHC. The second patient had a high ^{18}F -FDG uptake ($\text{SUV}_{\text{max}} = 9.2$), a high ^{18}F -FDG delta of 42.97%, no ^{68}Ga -RM2 binding and a negative GRP-R IHC.

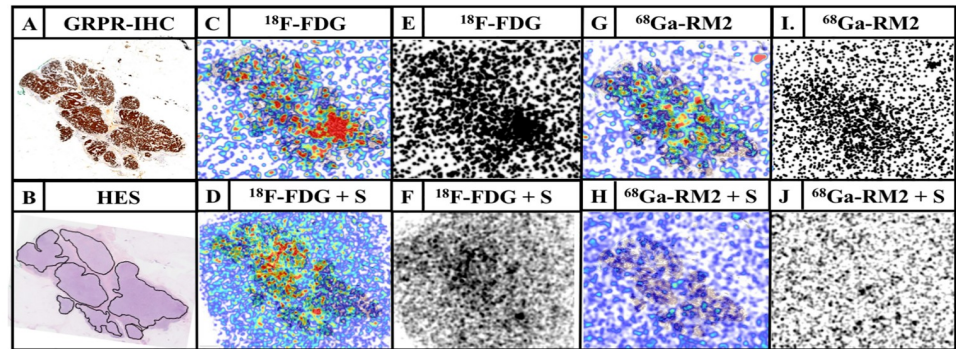


Fig 1. Example of a luminal B breast tumor sample. Representative GRP-R IHC (A; GRPR-IHC), HES staining (B; HES, black lines correspond to tumoral areas), ¹⁸F-FDG total binding fused with HES (C; ¹⁸F-FDG), ¹⁸F-FDG non-specific binding fused with HES (D; ¹⁸F-FDG + S), ¹⁸F-FDG total binding (E; ¹⁸F-FDG), ¹⁸F-FDG non-specific binding (F; ¹⁸F-FDG + S), ⁶⁸Ga-RM2 total binding fused with HES (G; ⁶⁸Ga-RM2), ⁶⁸Ga-RM2 non-specific binding fused with HES (H; ⁶⁸Ga-RM2 + S), ⁶⁸Ga-RM2 total binding (I; ⁶⁸Ga-RM2), ⁶⁸Ga-RM2 non-specific binding (J; ⁶⁸Ga-RM2 + S). S refers to the reference compound used (^{nat}F-FDG for ¹⁸F-FDG or ^{nat}Ga-RM2 for ⁶⁸Ga-RM2) to identify non-specific binding. In this sample, specific binding of ⁶⁸Ga-RM2 is strong and evident while specific binding of ¹⁸F-FDG was overall weak and heterogeneous.

<https://doi.org/10.1371/journal.pone.0210905.g001>

Discussion

The correlation between GRP-R overexpression in breast cancer and estrogen receptor positivity at protein level or mRNA level has been recently highlighted [2,3]. Moreover, it has been documented that when the breast primary is GRPR-positive, lymph node metastases also show GRPR overexpression [2,3]. Several clinical pilot studies have illustrated, *in vivo*, the potential of GRP-R for breast cancer imaging using radiolabelled GRP-R antagonists such as ⁶⁸Ga-SB3, ⁶⁸Ga-RM2 or ⁶⁸Ga-NOTA-RM26 [4,5,6]. In some of these studies it was shown that ER-positive tumors can be visualized with high contrast [5,6]. ¹⁸F-FDG PET/CT is also a valuable tool for staging of invasive breast cancer [10]. Highly ¹⁸F-FDG-avid tumors are generally Elston and Ellis grade 3, have a high proliferation index and negative hormone receptor status, while

Table 3. ⁶⁸Ga-RM2 and ¹⁸F-FDG bindings in breast cancer samples according to biological data.

Biological data	<i>n</i>	⁶⁸ Ga-RM2	¹⁸ F-FDG	<i>P</i> -value
<i>ER status</i>				
ER ⁺ (≥ 10%)	8	45.31 ± 13.23%	16.51 ± 28.45%	0.015
ER ⁻ (<10%)	6	14.32 ± 9.20%	20.21 ± 17.77%	0.483
<i>P</i>-value		0.030	0.479	
<i>PR status</i>				
PR ⁺ (≥ 10%)	6	43.29 ± 13.24%	21.71 ± 31.90%	0.089
PR ⁻ (<10%)	8	18.18 ± 18.43%	21.13 ± 18.24%	0.626
<i>P</i>-value		0.028	0.730	
<i>HER2 over-expression</i>				
Yes	3	16.13 ± 8.25%	30.19 ± 13.31%	0.200
No	11	32.25 ± 21.73%	18.98 ± 26.01%	0.163
<i>P</i>-value		0.280	0.269	
<i>Proliferation index Ki-67</i>				
High (≥20%)	10	20.62 ± 17.88%	25.77 ± 26.43%	0.783
Low (<20%)	4	49.24 ± 9.15%	10.40 ± 12.35%	0.029
<i>P</i>-value		0.023	0.287	

<https://doi.org/10.1371/journal.pone.0210905.t003>

Table 4. ¹⁸F-FDG SUV_{max} on PET/CT imaging in two breast cancer patients according to estrogen receptor (ER) expression, Ki-67 expression, ex vivo ¹⁸F-FDG and ⁶⁸Ga-RM2 bindings and GRP-R immunohistochemistry.

Patient	ER (%)	Ki-67 (%)	Molecular phenotype	¹⁸ F-FDG SUV _{max} [†]	¹⁸ F-FDG delta (%) [‡]	GRP-R IHC	⁶⁸ Ga-RM2 delta (%) [‡]
1	70	2	Luminal-A	2.5	0	Pos	37.46
2	90	30	Luminal-B	9.2	42.97	Neg	0

[†]: Data from ¹⁸F-FDG PET/CT

[‡]: Data from tissular micro-imaging experiments

<https://doi.org/10.1371/journal.pone.0210905.t004>

somewhat lower uptake can be encountered in low grade ER-positive tumors and in lobular carcinoma [10]. Indeed, imaging ER-positive breast tumors, especially the luminal-A phenotype, might be challenging using ¹⁸F-FDG PET/CT in some patients [11]. Therefore, how GRP-R imaging would perform compared to ¹⁸F-FDG in ER-positive breast cancer deserves investigation. We aimed to compare on breast cancer samples the binding of a radiolabelled GRP-R antagonist, ⁶⁸Ga-RM2, to that of ¹⁸F-FDG in order to better understand the potential of GRP-R imaging as a first step before a clinical study comparing the two tracers was launched.

Results of the present study on breast cancer samples showed that GRP-R targeting would be highly relevant in breast cancer, specifically in ER-positive tumors. Mean specific binding of ⁶⁸Ga-RM2 was 45.31 ± 13.23% in ER-positive tumors and only 14.32 ± 9.20% in ER-negative tumors (*P* = 0.030). The opposite pattern was noted as regards ¹⁸F-FDG bindings. As a result, the ratio of mean ⁶⁸Ga-RM2 binding to that of ¹⁸F-FDG binding in ER⁺ tumors was 3.42 vs 0.71 in ER⁻ tumors. Another important finding is the high ⁶⁸Ga-RM2 binding in tumors with low Ki-67 (49.24 ± 9.15%) while tumors with high Ki-67 exhibited lower ⁶⁸Ga-RM2 binding (20.62 ± 17.88%) (*P* = 0.023). Also, the ratio of mean ⁶⁸Ga-RM2 to ¹⁸F-FDG binding in tumors with low Ki-67 was significantly higher than in tumors with high Ki-67 (4.73 vs 0.80). Overall, these results suggest a role for GRP-R PET imaging that could be complementary or superior to ¹⁸F-FDG imaging in ER-positive tumors with a low proliferation index.

Thus, ¹⁸F-FDG PET/CT and GRP-R imaging may be complimentary for imaging breast cancer and more specifically so the ER-positive subtypes. A study comparing a GRPR targeting radiotracer and ¹⁸F-FDG for primary staging or for restaging recurrent breast cancer would be appreciated. Another approach that could enhance tumor detection, is the possibility of a multiple targeting as demonstrated by ⁶⁸Ga-BBN RGD that targets both GRP-R and integrin α_vβ₃. In a pilot study, this heterodimeric radiopharmaceutical performed better than ⁶⁸Ga-BBN (that targets only the GRP-R) in the detection of primary tumor and bone lesions in 11 patients [12]. Comparison with ¹⁸F-FDG would also be helpful for clinicians.

Finally, GRP-R targeting opens also attractive perspectives for radiopharmaceutical therapy of this subgroup of metastatic luminal patients with antagonists labelled with beta-emitters such as the lanthanides ¹⁷⁷Lu [13] or ¹⁶¹Tb [14, 15] or with alpha emitters.

Limitations of this study, apart the number of samples and its retrospective nature, is the ¹⁸F-FDG tissular micro-imaging which may appear questionable. Cristallographic studies at the human glucose transporter 1 (GLUT-1) revealed that glucose uptake is a 2-step mechanism involving glucose binding before active transport [16]. Moreover, enhanced ¹⁸F-FDG uptake in tumors is not only related to overexpression of glucose transporters but also to enhanced hexokinase activity which was not assessed here. Therefore, our ¹⁸F-FDG tissular micro-imaging is relevant (clear displacement of ¹⁸F-FDG with reference compound) and revealed at least the ¹⁸F-FDG binding site but may over-estimate or underestimate ¹⁸F-FDG uptake.

In total, our data point that GRPR targeting should be helpful for imaging breast cancer and more specifically so the ER-positive subtypes. A study comparing a GRPR targeting radio-tracer and ^{18}F -FDG for primary staging and for restaging recurrent breast cancer is clearly needed.

Supporting information

S1 Fig. ^{68}Ga -RM2 binding in ^{18}F -FDG-positive (^{18}F -FDG+) and ^{18}F -FDG-negative (^{18}F -FDG-) tumors.
(TIF)

Acknowledgments

Authors thank Life Molecular Imaging for the provision of the precursor RM2 and the reference compound ^{nat}Ga -RM2. Authors thank also CURIUM for the provision of ^{18}F -FDG. This work was funded by “La Ligue contre le Cancer Gironde 2016” and was performed under the context of the French Investment for the Future program within LabEx TRAIL ANR-10-LABX-57.

Author Contributions

Conceptualization: Clément Morgat.

Formal analysis: Clément Morgat, Romain Schollhammer.

Funding acquisition: Clément Morgat, Philippe Fernandez.

Investigation: Anne-Laure Cazeau.

Methodology: Clément Morgat, Romain Schollhammer, Nicole Barthe, Valérie Vélasco, Delphine Vimont, Elif Hindié.

Resources: Gaétan Macgrogan, Valérie Vélasco.

Software: Romain Schollhammer.

Supervision: Clément Morgat, Gaétan Macgrogan, Philippe Fernandez, Elif Hindié.

Writing – original draft: Clément Morgat.

Writing – review & editing: Clément Morgat, Romain Schollhammer, Gaétan Macgrogan, Delphine Vimont, Anne-Laure Cazeau, Elif Hindié.

References

1. Morgat C, Mishra AK, Varshney R, Allard M, Fernandez P, Hindié E. Targeting neuropeptide receptors for cancer imaging and therapy: perspectives with bombesin, neurotensin, and neuropeptide-Y receptors. *J Nucl Med.* 2014; 55(10):1650–7. <https://doi.org/10.2967/jnumed.114.142000> PMID: 25189338
2. Morgat C, MacGrogan G, Brouste V, Vélasco V, Sévenet N, Bonnefoi H et al. Expression of Gastrin-Releasing Peptide Receptor in Breast Cancer and Its Association with Pathologic, Biologic, and Clinical Parameters: A Study of 1,432 Primary Tumors. *J Nucl Med.* 2017; 58(9):1401–1407. <https://doi.org/10.2967/jnumed.116.188011> PMID: 28280221
3. Dalm SU, Sieuwerts AM, Look MP, Melis M, van Deurzen CH, Foekens JA, et al. Clinical Relevance of Targeting the Gastrin-Releasing Peptide Receptor, Somatostatin Receptor 2, or Chemokine C-X-C Motif Receptor 4 in Breast Cancer for Imaging and Therapy. *J Nucl Med.* 2015; 56(10):1487–93 <https://doi.org/10.2967/jnumed.115.160739> PMID: 26251419
4. Maina T, Bergsma H, Kulkarni HR, Mueller D, Charalambidis D, Krenning EP, et al. Preclinical and first clinical experience with the gastrin-releasing peptide receptor-antagonist [^{68}Ga]SB3 and PET/CT. *Eur J*

- Nucl Med Mol Imaging. 2016; 43(5):964–73 <https://doi.org/10.1007/s00259-015-3232-1> PMID: 26631238
5. Stoykow C, Erbes T, Maecke HR, Bulla S, Bartholomä M, Mayer S, et al. Gastrin-releasing Peptide Receptor Imaging in Breast Cancer Using the Receptor Antagonist ^{68}Ga -RM2 And PET. *Theranostics*. 2016 19; 6(10):1641–50 <https://doi.org/10.7150/thno.14958> PMID: 27446498
 6. Zang J, Mao F, Wang H, Zhang J, Liu Q, Peng L, et al. ^{68}Ga -NOTA-RM26 PET/CT in the Evaluation of Breast Cancer: A Pilot Prospective Study. *Clin Nucl Med*. 2018; 43(9):663–669. <https://doi.org/10.1097/RLU.0000000000002209> PMID: 30036253
 7. Wolff AC, Hammond ME, Hicks DG, Dowsett M, McShane LM, Allison KH, et al. Recommendations for human epidermal growth factor receptor 2 testing in breast cancer: American Society of Clinical Oncology/College of American Pathologists clinical practice guideline update. *J Clin Oncol*. 2013; 31(31):3997–4013. <https://doi.org/10.1200/JCO.2013.50.9984> PMID: 24101045
 8. Goldhirsch A, Winer EP, Coates AS, Gelber RD, Piccart-Gebhart M, Thürlimann B, et al. Personalizing the treatment of women with early breast cancer: highlights of the St Gallen International Expert Consensus on the Primary Therapy of Early Breast Cancer 2013. *Ann Oncol*. 2013; 24(9):2206–23. <https://doi.org/10.1093/annonc/mdt303> PMID: 23917950
 9. Maisonneuve P, Disalvatore D, Rotmensz N, Curigliano G, Colleoni M, Dellapasqua S, et al. Proposed new clinicopathological surrogate definitions of luminal A and luminal B (HER2-negative) intrinsic breast cancer subtypes. *Breast Cancer Res*. 2014; 16(3):R65. <https://doi.org/10.1186/bcr3679> PMID: 24951027
 10. Groheux D, Cochet A, Humbert O, Alberini JL, Hindié E, Mankoff D. ^{18}F -FDG PET/CT for Staging and Restaging of Breast Cancer. *J Nucl Med*. 2016; 57 Suppl 1:17S–26S.
 11. Humbert O, Berriolo-Riedinger A, Cochet A, Gauthier M, Charon-Barra C, Guiu S, et al. Prognostic relevance at 5 years of the early monitoring of neoadjuvant chemotherapy using ^{18}F -FDG PET in luminal HER2-negative breast cancer. *Eur J Nucl Med Mol Imaging*. 2014; 41(3):416–27. <https://doi.org/10.1007/s00259-013-2616-3> PMID: 24258007
 12. Zhang J, Mao F, Niu G, Peng L, Lang L, Li F, et al. ^{68}Ga -BBN-RGD PET/CT for GRPR and Integrin $\alpha\text{v}\beta\text{3}$ Imaging in Patients with Breast Cancer. *Theranostics*. 2018; 8(4):1121–1130. <https://doi.org/10.7150/thno.22601> PMID: 29464003
 13. Dumont RA, Tamma M, Braun F, Borkowski S, Reubi JC, Maecke H, et al. Targeted radiotherapy of prostate cancer with a gastrin-releasing peptide receptor antagonist is effective as monotherapy and in combination with rapamycin. *J Nucl Med*. 2013; 54(5):762–9 <https://doi.org/10.2967/jnumed.112.112169> PMID: 23492884
 14. Müller C, Zhernosekov K, Köster U, Johnston K, Dorrer H, Hohn A, et al. A unique matched quadruplet of terbium radioisotopes for PET and SPECT and for α - and β - radionuclide therapy: an in vivo proof-of-concept study with a new receptor-targeted folate derivative. *J Nucl Med*. 2012; 53(12):1951–9 <https://doi.org/10.2967/jnumed.112.107540> PMID: 23139086
 15. Hindié E, Zanotti-Fregonara P, Quinto MA, Morgat C, Champion C. Dose Deposits from ^{90}Y , ^{177}Lu , ^{111}In , and ^{161}Tb in Micrometastases of Various Sizes: Implications for Radiopharmaceutical Therapy. *J Nucl Med*. 2016; 57(5):759–64. <https://doi.org/10.2967/jnumed.115.170423> PMID: 26912441
 16. Mueckler M, Makepeace C. Model of the exofacial substrate-binding site and helical folding of the human Glut1 glucose transporter based on scanning mutagenesis. *Biochemistry*. 2009; 48(25):5934–42 <https://doi.org/10.1021/bi900521n> PMID: 19449892